HHS Public Access

Author manuscript

Sci Transl Med. Author manuscript; available in PMC 2020 July 30.

Published in final edited form as:

Sci Transl Med. 2016 July 27; 8(349): 349ra101. doi:10.1126/scitranslmed.aaf4964.

Noninvasive low-level laser therapy for thrombocytopenia

Qi Zhang[1,2], **Tingting Dong**[1,2], **Peiyu Li**[1,2], **Mei X. Wu**[1,2,3,*]

[1]Wellman Center for Photomedicine, Massachusetts General Hospital, Boston, MA 02114, USA.

[2]Department of Dermatology, Harvard Medical School, Boston, MA 02114, USA.

[3]Affiliated faculty member of the Harvard-MIT Division of Health Sciences and Technology, Cambridge, MA 02115, USA.

Abstract

Thrombocytopenia is a common hematologic disorder that is managed primarily by platelet transfusions. We report here that noninvasive whole-body illumination with a special near-infrared laser cures acute thrombocytopenia triggered by γ-irradiation within 2 weeks in mice, as opposed to a 5-week recovery time required in controls. The low-level laser (LLL) also greatly accelerated platelet regeneration in the presence of anti-CD41 antibody that binds and depletes platelets, and prevented a severe drop in platelet count caused by a common chemotherapeutic drug. Mechanistically, LLL stimulated mitochondrial biogenesis specifically in megakaryocytes owing to polyploidy of the cells. LLL also protected megakaryocytes from mitochondrial injury and apoptosis under stress. The multifaceted effects of LLL on mitochondria bolstered megakaryocyte maturation; facilitated elongation, branching, and formation of proplatelets; and doubled the number of platelets generated from individual megakaryocytes in mice. LLL-mediated platelet biogenesis depended on megakaryopoiesis and was inversely correlated with platelet counts, which kept platelet biogenesis in check and effectively averted thrombosis even after repeated uses, in sharp contrast to all current agents that stimulate the differentiation of megakaryocyte progenitors from hematopoietic stem cells independently of platelet counts. This safe, drug-free, donor-independent modality represents a paradigm shift in the prophylaxis and treatment of thrombocytopenia.

*Corresponding author. mwu5@mgh.harvard.edu.

Author contributions: Q.Z. designed and performed all experiments, analyzed the data, performed statistical analysis, and wrote the manuscript; T.D. performed confocal microscopy, animal treatment, and flow cytometric analysis; P.L. performed genotyping, real-time PCR, and related flow cytometry experiments of *Pgc1a*$^{+/-}$ mice; and M.X.W. designed and supervised the overall project and wrote the manuscript.

SUPPLEMENTARY MATERIALS

www.sciencetranslationalmedicine.org/cgi/content/full/8/349/349ra101/DC1

Competing interests: M.X.W. and Q.Z. have filed a U.S. utility patent of “Systems and methods for enhancing platelet biogenesis and extending platelet lifespan, in circulation and in storage, with low level light.” The authors declare that they have no other competing interests.

Data and materials availability: All relevant data are reported in the article and the Supplementary Materials. All materials are available commercially or can be derived using methods described in this study.

INTRODUCTION

Thrombocytopenia is responsible for uncontrollable bleeding and death owing to an abnormally low number of platelets in the blood. The disease is mostly managed by platelet transfusion, which is associated with a variety of complications (including infections, allergic reactions, platelet refractoriness, fever, and immunosuppression) and limited only to patients with life-threatening conditions. Considerable progress has been made in the development of therapeutic agents for treating thrombocytopenia in the past three decades. For instance, recombinant human interleukin-11 (rHuIL-11) is currently used for chemotherapy-induced thrombocytopenia, and thrombopoietin (TPO) receptor agonists romiplostim and eltrombopag are in the clinic for chronic immune thrombocytopenia (ITP), both of which were approved by U.S. Food and Drug Administration in 1997 and 2008, respectively. Almost all of these agents augment the growth and differentiation of hematopoietic stem cells (HSCs) and/or progenitor cells, increasing megakaryopoiesis independently of the number of circulating platelets (1). Hence, a high dose of these agents often causes a deleterious thrombosis, whereas a low dose exhibits modest or little effect (2), which severely limits their broad clinical applications. An effective modality that promotes platelet production with minimal risk of thrombosis remains an urgent and unmet medical need for management of thrombocytopenia.

Blood platelets are small, anucleate cells generated from megakaryocytes (MKs) that reside primarily in the bone marrow (BM). The cells are differentiated from HSCs and represent the largest (an average diameter of 50 to 100 μm) and also one of the rarest cells, consisting of only ~0.05% of BM nucleated cells under physiological conditions (3), but the cells grow exponentially in number in patients suffering thrombocytopenia (4). During MK maturation, multiple rounds of nuclear proliferation take place in the absence of cell division, in a process called endomitosis, through which their cytoplasm is extensively enlarged and genomic DNA is amplified up to 64N in humans or 256N in mice, concurrent with synthesis of abundant cytoskeletal proteins, platelet-specific granules, and invaginated membrane systems. The cellular enlargement is followed by proplatelet formation in which the terminal mature MKs convert their entire cytoplasm into many long, branching proplatelets that are elongated at a rate of ~1 μm/min to reach the length of 250 to 500 μm over a few hours (5). The massive cytoplasm remodeling and vigorous protrusion and elongation of proplatelets are driven by microtubule forces and rely heavily on adenosine 5′-triphosphate (ATP) generation (6, 7), implicating a central role for mitochondria in the process. Consistent with this, ultrastructural abnormalities and inadequate function of MK mitochondria are sometimes associated with impaired thrombopoiesis in ITP and some myelodysplastic syndrome (MDS) patients (8, 9). Point mutations in mitochondrial cytochrome c cause dysregulated platelet formation and thrombocytopenia in humans (10), suggesting that platelet biogenesis is sensitive to mitochondrial activity. We recently showed that inadequate mitochondrial function predisposed mice lacking immediate early responsive gene X-1 (IEX-1) to thrombocytopenia upon stress (11). One of the major functions of IEX-1 is to enhance ATP synthase activity at the mitochondrial respiratory chain (12), and its null mutation compromises ATP generation and increases the production of reactive oxygen species (ROS) in mitochondria (13). The ability of mitoquinone, a mitochondrion-specific

antioxidant, to completely reverse thrombocytopenia in IEX-1–deficient mice suggests that mitochondrial functions are crucial in platelet generation (14).

A special near-infrared laser with a relatively low energy density, called low-level laser (LLL) or cold laser, can activate cytochrome c oxidase in the mitochondrial respiratory chain and improve mitochondrial function (15, 16). LLL appears to be able to directly increase mitochondrial membrane potential (17), stimulate ATP synthesis (16), and modulate cellular ROS and Ca^{2+} levels (18, 19). LLL can also attenuate oxidative stress (20), prevent apoptosis of various cells (19), reduce inflammation (16), and promote proliferation and differentiation of mesenchymal and cardiac stem cells, dental pulp stem cells, adipose-derived stem cells, and various progenitor and stem cells (21). The light illumination modulates other signaling transduction pathways as well secondarily to more efficient function of mitochondria under various conditions of stress (22). Because of its known effects on mitochondria, we hypothesized that LLL might have a beneficial effect on platelet generation.

We demonstrate here that noninvasive whole-body LLL illumination increases platelet generation and completely cures or greatly ameliorates thrombocytopenia caused by γ-irradiation (IR), ITP (induced by anti-CD41 antibody), or chemotherapy in mice. LLL primarily targeted MKs and bolstered mitochondrial biogenesis specifically in polyploid MKs, but not in diploid cells, even though LLL increased ATP production transiently in MKs, HSCs, and BM nucleated cells. These findings support LLL as a new prophylactic and therapeutic modality to manage thrombocytopenia with a low risk of thrombosis.

RESULTS

LLL accelerates proplatelet formation and enhances platelet production from MKs

To explore possible effects of LLL on platelet biogenesis, we sorted mature MKs from mouse BM nucleated cells on the basis of $CD41^+$ and high forward scatter (FSC^{high}) (23), and exposed them to 810-nm diode laser for varying durations (Fig. 1A). The sorted MKs were then cultured for 1 hour in serum-free expansion medium containing TPO (100 ng/ml)—called MK medium hereafter. LLL at energy densities ranging from 1 to 10 J/cm^2 significantly enhanced ATP synthesis in MKs, with the most prominent effect at 3 to 5 J/cm^2 (Fig. 1B). The laser at 3 J/cm^2 was thus selected for subsequent ex vivo studies unless otherwise indicated. We first treated the sorted MKs with LLL or a soft white light-emitting diode (LED) as sham light and cultured them in MK medium for 24 hours, followed by flow cytometric analysis of the size of 5000 MKs by FSC on the gate of $CD41^+$ cells, which revealed an average 60% increase in LLL-treated MKs, in comparison with only a 37% size increase in sham-treated MKs (Fig. 1C). LLL increased the major diameter of the MKs by 76% after 24-hour culture, as opposed to only 39% increase in the absence of LLL under similar conditions (Fig. 1D).

Apart from cell enlargement, LLL-treated MKs had already generated invaginated membrane systems throughout the entire cytoplasm after 24-hour culture, whereas little such membrane system was formed in control MKs (Fig. 1D), suggesting that LLL accelerates MK maturation. The invaginated membrane system is the membrane reservoir of

proplatelets and one of the key determinants of the number of platelets generated from each MK (24). In accordance with this, LLL-treated MKs produced twice as many platelets as control MKs (Fig. 1E), owing to an increased proportion of large proplatelet-forming MKs (PPF-MKs) (Fig. 1, F and G).

PPF-MKs were tracked in culture for 24 hours under phase-contrast microscopy, during which MKs converted their cytoplasm into many proplatelets that were decorated with multiple protrusions, adopting a blossom-like morphology at varying sizes (Fig. 1F). About 23.5% of $CD41^+$ FSC^{high} MKs formed large PPF-MKs with a cell diameter of ≥100 μm in the absence of LLL. Strikingly, the percentage of these large PPF-MKs increased to 42.7% in the presence of LLL, representing a more than 80% increase compared to controls (Fig. 1G). To recapitulate this finding in vivo, mature MKs were sorted, treated with LLL or sham light, labeled with vital fluorescent dye carboxyfluorescein diacetate succinimidyl ester (CFSE), and intravenously infused into recipient mice (11). LLL-treated MKs generated higher levels of platelets than control counterparts from day 2 to day 5 after infusion in recipients (Fig. 1H).

Mitochondrial ATP production is crucial in platelet formation

Further investigation revealed significant correlations between MK ATP levels measured at 1 hour after LLL and platelet counts measured 3 days later (Fig. 2A). LLL-mediated enhancement of platelet generation was severely blunted by oligomycin A (OA) (Fig. 2B)—an antibiotic that specifically inhibits mitochondrial F_1F_0-ATP synthase and reduces ATP synthesis in cells, which correlated with OA-mediated inhibition of ATP production in MKs (Fig. 2C). The importance of ATP in platelet formation is consistent with the development of irreversible thrombocytopenia upon stress in mice lacking IEX-1 (11). MKs lacking IEX-1 had reduced mitochondrial membrane potential ($\Delta\psi_m$) (Fig. 2D) and ATP production (Fig. 2E) compared with wild-type controls. Proplatelet differentiation from IEX-1 knockout (KO) MKs was severely hindered, forming fewer and shorter proplatelet branches of less complexity (Fig. 2F).

The average size of IEX-1 KO PPF-MKs was halved as compared with wild-type PPF-MKs (Fig. 2G), confirming a pivotal role of mitochondrial activity in proplatelet formation. Remarkably, a single dose of LLL rescued ATP levels in IEX-1 KO MKs (Fig. 2E) and restored proplatelet formation, leading to a near-normal PPF-MK morphology 24 hours after illumination (Fig. 2F). The average diameter (±SEM) of IEX-1 KO PPF-MKs was only 67.0 ± 17.8 μm but increased to 97.6 ±31.3 μm after LLL treatment—a 46% increase—although they were still smaller than wild-type PPF-MKs (Fig. 2G). LLL-mediated enlargement of KO PPF-MKs translated into a twofold increase in the number of platelets produced when compared to sham treatment in the 3-day culture (Fig. 2H). These data corroborate mitochondrial activity as a determinant factor of platelet production.

LLL bolsters mitochondrial biogenesis in MKs

We next determined how brief (3 min and 20 s) LLL treatment of MKs in vitro could affect platelet differentiation for days. We found that LLL elevated ATP production in MKs only briefly, peaking at 60 min and returning to the basal level in 90 min (Fig. 3A). This transient

and robust ATP production was also evidenced in BM nucleated cells, and HSCs and progenitor cells [$Lin^{-}Sca1^{+}cKit^{+}$ cells (LSKs)] after LLL treatment (Fig. 3A). However, to our surprise, LLL-facilitated mitochondrial biogenesis occurred only in MKs, not in LSKs or BMs, as indicated by doubling mitochondrial content only in MKs 24 hours after LLL compared to controls (Fig. 3B). A mitochondrial mass increase was confirmed by the relative ratio of mitochondrial DNA to nuclear DNA (Fig. 3C).

LLL-mediated mitochondrial biogenesis was further corroborated at the molecular level. Peroxisome proliferator–activated receptor-γ coactivator 1α (*Pgc1a*) is a master regulatory gene for mitochondrial biogenesis (25, 26). Its expression was robustly enhanced 4 hours after LLL in MKs, after which other genes associated with mitochondrial biogenesis were also up-regulated significantly (Fig. 3D and table S1), including mitochondrial transcriptional factor A (*Tfam*), dynamin-related protein (*Drp1*), mitochondrial fission 1 protein (*Fis1*), and mitochondrial fission factor (*Mff*). A role for *Pgc1a* expression in LLL-mediated platelet biogenesis was corroborated by MKs sorted from $Pgc1a^{+/-}$ mice. MKs from $Pgc1a^{+/-}$ mice expressed a half amount of *Pgc1a* transcript as that of wild-type MKs (fig. S1A). After treatment with LLL, mitochondrial mass increased by 87% in wild-type MKs but only 10% in $Pgc1a^{+/-}$ MKs (fig. S1B). Consequently, LLL raised platelet production by 100% in wild-type MKs as opposed to only 20% in $Pgc1a^{+/-}$ MKs (fig. S1C). The results indicate an important role for PGC-1a in LLL-mediated mitochondrial biogenesis and platelet formation. *Pgc1a* expression was low in BM nucleated cells and LSKs, but elevated by LLL treatment (fig. S2A), corroborating the ability of LLL to stimulate *Pgc1a* in different cell types (27). However, in contrast to MKs, none of the genes downstream of *Pgc1a* (26)—*Tfam*, *Drp1*, *Fis1*, or *Mff*—were up-regulated in BM nucleated cells or LSKs measured in parallel (fig. S2B), similar to what has been described previously (27), probably owing to diploidy of the cells in contrast to the polyploidy of MKs (fig. S2C) (28).

To determine the role of MK polyploidy in LLL-mediated biogenesis of mitochondria, we sorted $CD41^{+}$ MKs from BM nucleated cells on the basis of DNA content (29). The fraction of 2N/4N cells contained an average of 2.3N MKs, like diploid cells, whereas the fraction of ≥8N cells contained an average of 11.4N MK cells, considered to be polyploid MKs (Fig. 3E). MKs with ≥8N DNA responded to LLL much stronger than did those with 2N/4N, manifested by substantial increases in mitochondrial biogenesis and *Pgc1a* expression in polyploid MKs over diploid MKs under similar conditions (Fig. 3, F and G). The DNA copy number–dependent effect of LLL was even more predominant in the expression of downstream genes *Tfam*, *Drp1*, *Fis1*, and *Mff*, with 100 to 200% increases of these genes in polyploid MKs but only 0 to 20% increases in diploid MKs (Fig. 3H). In accordance with this, LLL enhanced platelet production by 200% over sham light in polyploid MKs, but only 29% in diploid MKs (Fig. 3I). Thus, LLL enhances mitochondrial biogenesis efficiently in polyploid MKs but not in diploid cells.

The increase in mitochondrial mass was observed in multi-nucleated MKs (Fig. 3, J and K), where mitochondria were counted only in multinuclear cells before the invaginated membrane system was fully developed. Apart from an increased number of mitochondria, LLL also altered mitochondrial distribution in MKs. Mitochondria were more evenly

distributed over the entire cells after LLL, whereas mitochondria in sham-treated MKs were concentrated primarily around the perinuclear region (Fig. 3J). Measurement of distances of individual mitochondria to the nearest nucleus revealed that 16% of mitochondria in LLL-treated MKs were located >4 μm away from the nucleus, whereas these mitochondria away from the nucleus were only 4% in control MKs (Fig. 3L).

LLL cures thrombocytopenia induced by IR fast

To explore any therapeutic possibility for LLL, we first determined a laser dose that could sufficiently penetrate through mouse skin, muscle, and bone layers, reaching the BM at 3 J/cm^2. Among several lasers tested, including a 660-nm continuous wave laser, 810-nm pulsed lasers (10 and 100 Hz), and an 810-nm continuous wave laser, the latter showed the most effective transmittance, with 9.0 ±0.6% of the laser power being transmitted into the BM (Fig. 4A). Thus, whole-body illumination for 5 min with 810-nm continuous wave laser at 100 mW/cm^2 or an energy density of 30 J/cm^2 was selected so that the mouse BM nucleated cells could receive an energy density of ~3 J/cm^2, equivalent to the laser energy used in our ex vivo culture experiments. Laser penetration was verified by increased ATP production in BMs isolated from the mouse vertebrae, femur, tibia, and pelvis 1 hour after whole-body LLL illumination (Fig. 4B). The effect of LLL on MK differentiation in vivo was subsequently confirmed by confocal microscopy in femur bones, where blood vessels and MKs were stained for CD105 and CD41, respectively (Fig. 4C). Large blossom-like MKs, likely PPF-MKs, were readily seen all over the BM 24 hours after LLL, whereas such blossom-like cells were hardly found in the BM of control mice (Fig. 4C). About 36% of MKs in LLL-treated femurs formed PPF-MKs, whereas only 19% of MKs formed PPF-MKs in control femurs (Fig. 4D).

The aforementioned study suggested that LLL mainly targeted MKs and thus should have greater impact in subjects with a high number of MKs, like those suffering from thrombocytopenia, because the disorder triggers compensatory megakaryopoiesis. We therefore induced thrombocytopenia by 3-Gy IR and then treated the mice with whole-body LLL illumination for 5 min per day at an energy density of 30 J/cm^2 using the following protocols: (i) treated once at 6 hours after IR (IR + 1×LLL), (ii) treated twice at 6 and 24 hours after IR (IR + 2×LLL), and (iii) treated four times for four consecutive days starting at day 0 (IR + 4×LLL). Completed blood counts were checked weekly and compared with γ-irradiated mice receiving sham light. There were no significant alterations in the counts of white blood cells, lymphocytes, monocytes, granulocytes, or red blood cells in the presence of LLL or sham light throughout the entire experimental period (Fig. 5A). However, platelet recovery was much faster in the mice in a laser dose-dependent fashion (Fig. 5B). The platelet counts reached a pre-IR level or above as early as 2 weeks (IR + 4×LLL) or 3 weeks (IR + 2×LLL) after IR, as opposed to 5 weeks of sham-treated mice (IR).

Consistent with a rising platelet count was normalization of tail bleeding time (Fig. 5C) as well as mean platelet volume (Fig. 5D) in the mice when examined 2 weeks after IR. Platelets produced in 4×LLL-treated mice were ultrastructurally indistinguishable from normal control platelets containing comparable levels of granules, mitochondria, and open canalicular systems (Fig. 5E). In contrast, platelets isolated from γ-irradiated mice exhibited

abnormal morphology—two- to threefold bigger than a normal platelet—with lower amount of mitochondria and granules (Fig. 5E). The abnormal morphology of platelets may explain the doubled bleeding time in these mice compared to normal controls despite only a 40% drop in platelet count (Fig. 5, B and C). The overall aggregation activity of platelets isolated from 4×LLL-treated mice was also identical to that of normal controls receiving no IR (Fig. 5F). These results indicate that platelets generated by LLL treatment remained intact morphologically and functionally.

Furthermore, although LLL significantly augmented platelet production in thrombocytopenic mice, there was no significant effect on platelet counts in normal mice when LLL was administered once every other day for up to 12 days as compared to sham-treated mice (Fig. 5G). There were also no significant alterations in the number of MKs (Fig. 5G), which supports the safety of this approach, as there would be little concern about thrombosis even after repeated LLL uses.

Apart from enhancement and acceleration of proplatelet formation, LLL might also protect MKs from apoptosis induced by IR, leading to a higher number of MKs in LLL-treated versus sham-treated mice during the first 3 days after IR. The number of MKs peaked 2 days after IR and rose from 37,353 to 78,159 in one femur bone in the presence of LLL, which was about 50% higher than that in the absence of LLL (Fig. 5H). When MKs were sorted and subjected to 3-Gy IR followed by measurement of caspase-3/7 activation (fig. S3A), a threefold increase in caspase-3/7 activity was attained, on average, in γ-irradiated MKs relative to non-IR counterparts (fig. S3B), concurrent with marked decreases in cell viability within 24 hours after IR (fig. S3C). LLL given at 6 hours after IR significantly inhibited caspase-3 activation and enhanced cell survival of γ-irradiated MKs.

LLL-mediated protection of MKs from IR-induced damage resulted in an increasing percentage of total PPF-MKs from 20.5 to 30.2%, especially the percentage of large PPF-MKs (from 5.8 to19.2%) (fig. S3D), as well as restoration of platelet production of γ-irradiated MKs cultured ex vivo (fig. S3E). Notably, an initial increase in the number of MKs was followed by a sharp decline to the lowest level on day 5 after IR (Fig. 5H). However, the number of MKs rose again steadily in LLL-treated mice, whereas it continued to drop in sham-treated mice (Fig. 5H), which might be attributed to better differentiation of MKs from HSCs in response to LLL, although a further study would be required to reach this conclusion.

LLL mitigates thrombocytopenia induced by anti-CD41 antibodyor 5-fluororacil

We investigated whether LLL-mediated thrombopoiesis was specific for thrombocytopenia induced by IR or whether it induced platelet biogenesis in other forms of thrombocytopenia commonly seen in the clinic. We depleted platelets by administering anti-CD41 antibody daily for 7 days to create an animal model of ITP (30). ITP mice were treated with either sham light or LLL at 30 J/cm^2 daily with an initial illumination on day 3 when platelet counts had reached a nadir (Fig. 6A). With only 2 days of therapy, LLL accelerated the recovery of platelet counts in the presence of anti-CD41 antibody, although platelet counts rebounded in all of the mice by day 7, owing to compensatory thrombopoiesis (Fig. 6A). Bleeding time was also normalized on day 5 in LLL-treated animals (Fig. 6B). Similar

effects of LLL on platelet regeneration were seen in mice receiving the common chemotherapeutic drug 5-fluororacil (5-FU). In this model, LLL was given once daily from day 0 to day 2. The chemotherapeutic drug diminished circulating platelet counts by 43% on day 4 at a dose of 150 mg/kg body weight (31), but three doses of LLL were sufficient to alleviate thrombocytopenia (Fig. 6C) and normalize bleeding time on day 4 (Fig. 6D) in the drug-treated mice, although all miced recovered again by day 8.

LLL displays thrombopoietic potentials in human cells

We assessed the clinical potential for LLL therapy by stimulating platelet production in human MKs. $CD34^+$ cells were cultured in serum-free expansion medium containing human TPO (100 ng/ml), which recapitulated all of the differentiation stages of megakaryopoiesis described previously (32). In the culture, $CD34^+$ cells differentiated predominantly into MK progenitors in 6 days, MKs in 12 days, and platelets in 15 days (Fig. 7A). We sorted MKs from day 12 cultures and treated them with LLL at various energy densities. ATP production in human MKs was significantly stimulated by LLL at energy densities ranging from 0.5 to 10 J/cm^2, with a peak response at 3 J/cm^2 (Fig. 7B), resembling mouse MKs (Fig. 1B).

The same laser power as used in mice (3 J/cm^2) was administered on day 0 (to mainly $CD34^+$ cells in the culture), day 6 (to MK progenitors), or day 12 (to MKs), followed by evaluation of the platelet production on day 15. MK differentiation in these cultures was verified by an increasing polyploidy over time, with a maximal percentage of polyploid cells (≥8N) on day 12 (Fig. 7C). The increases in cellular polyploidy correlated with the effect of LLL on platelet production, with the highest level of platelets induced by LLL on day 12 of the culture (Fig. 7D). The results suggest that MKs are the preferential target of LLL, as seen in mice, and that LLL has similar effects on platelet biogenesis in human and mouse MKs.

DISCUSSION

We demonstrated that noninvasive LLL illumination could robustly increase platelet generation in thrombocytopenic mice, but not in normal controls. The laser worked equally well in both human and mouse MKs ex vivo, consistent with evolutionary conservation of mitochondria and thrombopoiesis between these two species. These observations argue for the translational potential of LLL as both a therapeutics and a preventative modality for thrombocytopenia. The most important finding of the study is that LLL targets primarily MKs, which keeps thrombopoiesis in check by free plasma TPO that is inversely correlated with the number of circulating platelets (33). In sharp contrast, all current agents used in the clinics or under the development for treating thrombocytopenia promote the differentiation of MK precursors from HSCs independently on platelet counts, thereby imposing a high risk of thrombosis if used at a high dose.

Because the number of MKs is reciprocally regulated by platelet counts via megakaryopoiesis, the more severe the thrombocytopenia, the more vigorous megakaryopoiesis would be induced, bringing about a great number of MKs, and the more prominent effect of LLL on thrombopoiesis could occur. In contrast to thrombocytopenic condition, LLL displays little effect on platelet counts under a physiological condition or

when the platelet counts return to a normal level because of an extremely low number of MKs in these healthy subjects. We examined three different rodent models of acquired thrombocytopenia—IR-, ITP-, and 5-FU–induced—but in theory, LLL should benefit all patients with acquired thrombocytopenia regardless of its etiology, provided that megakaryopoiesis is triggered by the thrombocytopenia. It is not clear, however, whether LLL has similar effects on inherent thrombocytopenia or MDS, which should be investigated separately because it will require a large number of BM samples from many patients to find a few of them with a defect in mitochondrial functions for the evaluation. Patients with inherent thrombocytopenia and MDS are caused by a variety of etiologies, such as a mitochondrial defect, which consists of a small fraction of the patients (8, 9). Nevertheless, a combination of LLL with rHuIL-11, romiplostim, or eltrombopag may additively or synergistically augment platelet biogenesis and reduce dose-dependent side effects of these agents, thus extending the application of these agents to some of the inherent thrombocytopenia or MDS (2), because these agents target early stages of thrombopoiesis that are distinct from LLL. To date, there is no agent, to the best of our knowledge, that specifically targets proplatelet formation or downstream of megakaryopoiesis.

The mechanism underlying LLL-mediated thrombopoiesis relies primarily on its unique effects on mitochondria. LLL protected MKs from apoptosis induced by a mitochondrion-dependent pathway like IR as has been demonstrated by a number of studies (34). Next, LLL specifically augmented mitochondrial biogenesis in MKs, which has never been shown in other types of cells and is ascribed to a polyploidy of MKs, a unique character of MKs. A previous study demonstrated that near-infrared light exposure increased *Pgc1a* expression by about 20% in mouse muscle cells, but expression of the downstream mitochondrial component genes (*Tfam*, *Nrf-1*, *Sirt3*,and *cytochrome c*) was unaltered (27). Likewise, LLL increased *Pgc1a* transcription in BMs and LSKs, concomitant with no mitochondrial biogenesis or increases in expression of other downstream genes. This unique effect of LLL on mitochondrial biogenesis in polyploid MKs is consistent with functional amplification of MK genome required for increasing synthesis of proteins in association with platelet function in parallel with cell enlargement (28). The specific MK effect of LLL explains why LLL profoundly affects MKs while having little impact on BM nucleated cells, LSKs, lymphocytes, and red blood cells under similar conditions.

The ability of LLL to increase MK mitochondrial biogenesis and mitochondrial activity is likely to be essential in its thrombopoietic effect (35), deduced from a correlation between ATP production and platelet generation. A high energy demand during proplatelet formation is also consistent with in vivo platelet biogenesis in which MKs migrate toward BM sinusoids during proplatelet formation, where oxygen levels are elevated to secure a great deal of mitochondrial oxidative phosphorylation (36); this is in contrast to HSCs that reside predominantly in low-oxygen niches in the bones (37). Likewise, MKs tend to form proplatelets in pulmonary capillary that also contains higher levels of oxygen (38). In contrast, inadequate activity of mitochondria lacking IEX-1 hinders proplatelet formation, which could be normalized by LLL treatment. Direct evidence of ATP importance in proplatelet formation comes from the studies of Richardson *et al.* (6, 7), where they showed that ATP activated proplatelet elongation and significantly enhanced proplatelet growth.

Thus, ATP is likely a rate-determining factor in the late stage of thrombopoiesis, providing further insight into how platelet production can be enhanced both in vitro and in vivo.

LLL therapy has been routinely used in the clinics for analgesic, anti-inflammation, and wound healing for more than two decades with a long record of safety. This safe, drug-free, and donor-independent modality can be readily adopted by most practitioners as a standalone or complement treatment of thrombocytopenia. Currently, no LLL device can simultaneously illuminate a majority of human BM (whole body) with sufficient laser energy of 3 J/cm^2. Such a device will be needed to noninvasively enhance platelet biogenesis in large animals and subsequent clinical trials in the future. It is worthwhile to emphasize that this modality is not intended to replace platelet transfusions in the management of bleeding, but rather to greatly reduce the need of platelet transfusion and offer prophylaxis and therapeutics of thrombocytopenia.

MATERIALS AND METHODS

Study design

The study aimed at determining the effects of LLL on platelet biogenesis and its therapeutic and prophylactic potentials for thrombocytopenia. We hypothesized that LLL could enhance platelet biogenesis in light of its ability to augment mitochondrial activity. For all ex vivo studies, we used primary MKs from mouse BMs or human CD34$^+$ cell–derived cultures. The effect of LLL was evaluated by LLL-mediated increases of ATP content, mitochondrial mass, proplatelets or platelets of MKs, and mitochondria-related gene expression. The number of experiments (including biological and technical replicates) is defined in each figure legend. For in vivo experiments, three different mouse models were tested to validate the ability of LLL to cure or ameliorate thrombocytopenia induced by IR, immune depletion (ITP), and 5-FU (chemotherapy), which comprise most of the acquired thrombocytopenia seen in the clinic. All mice were randomly divided to different experiment groups, and the numbers of mice are outlined in each figure legend. The end point is either the moribundity for mice or a loss of body weight more than 15% in accordance with Institutional Animal Care and Use Committee guidelines. The sample size was determined using power analysis to give a statistical power of >90% and SD of 0.1 based on the expected experiment result at α =0.05. Investigators were blinded to all cell and mouse treatment groups. All outliers of study subjects were included in the data analysis.

Mice

Pgc1a$^{+/-}$ and C57BL/6 mice of either gender at 8 to 12 weeks of age were purchased from the Jackson Laboratory. Wild-type and *IEX-1* KO mice on a 129Sv/C57BL/6 background were generated in our laboratory (16). ITP was induced by daily intraperitoneal injection of anti-CD41 antibody (BD Biosciences) for a total of 8 days at 0.1 mg/kg body weight per day. For chemotherapy-induced thrombocytopenia, mice were treated once by intraperitoneal injection of 5-FU (Sigma) at 150 mg/kg body weight. IR at 3 Gy was performed using a ^{137}Cs γ-irradiator (Mark I, model 30, J.L. Shepherd). The animal protocols were approved by the subcommittee on Research Animal Care of the

Massachusetts General Hospital, according to the National Institutes of Health *Guide for the Care and Use of Laboratory Animals*.

LLL treatment

For ex vivo illumination, 810-nm diode laser (PhotoThera) was set as continuous wave with a power density of 15 mW/cm^2 for 3 min and 20 s to obtain an energy density of 3 J/cm^2. For whole-body LLL illumination, a hair-removed mouse was placed in a light-transparent, small plastic box and positioned under the laser lens that covered the whole trunk and limbs. The power density of LLL was 100 mW/cm^2, with a total exposure time of 5 min to obtain an energy density of 30 J/cm^2. The first dose of LLL was given at 4 to 6 hours after IR or 5-FU treatment or 3 days after the first anti-CD41 antibody injection. Sham light was administered with a small soft white LED light bulb (3 W, A15) from General Electric. To measure the laser power transmission, fresh skin, muscle, and vertebral bone layers were removed immediately after mice were sacrificed and exposed to varying lasers. The penetrated light was measured by a laser power meter (Ophir Nova II), and a difference in light power on the surface of the skin and beneath the bone layer was calculated as a transmittance rate (%).

Fluorescence-activated cell sorting

MouseBMswereincubatedwithanti-CD41–allophycocyanin(BioLegend), and mature MKs were sorted on a FACSAria (BD Biosciences) on the basis of CD41$^+$ FSC^{high}. Alternatively, mouse BMs were incubated first with anti-CD41–FITC and 10 μM Hoechst 33342 (Sigma). MKs were sorted into 2N/4N and ≥8N fractions as previously described (29). Details and additional methods are provided in Supplementary Materials and Methods.

Human MK and platelet cultures

Frozen human CD34$^+$ cells were obtained from STEMCELL Technologies and differentiated in serum-free expansion medium supplemented with human TPO (100 ng/ml) (PeproTech) (32). During the culture, megakaryocytic differentiation stages were routinely evaluated by May-Grünwald-Giemsa staining (Sigma) and CD41 levels via flow cytometry. CD34$^+$ cells, MK progenitors, mature MKs, or platelets were collected on day 0, 6, 12, or 15 of the culture, respectively.

Statistical analysis

Data are presented as means ± SEM. Statistical significance was assessed with two-tailed Student's *t* test for comparison between two groups or one-way ANOVA for multiple group comparison. A value of $P < 0.05$ was considered statistically significant. The relationship between ATP level and platelets was tested by regression and correlation analysis, and coefficient of determination (R^2) was calculated. All statistical analyses were performed using GraphPad Prism 6.0 (GraphPad Software).

Supplementary Material

Refer to Web version on PubMed Central for supplementary material.

Acknowledgments:

We thank M. Hamblin, D. Kuter, and R. Anderson (Massachusetts General Hospital) for their stimulating comments and discussions, and the staff at the Photopathology Core at Wellman Center for Photomedicine for fluorescence-activated cell sorting and electron microscopy assistance.

Funding: This study was supported in part by FA9550-13-1-0068, Department of Defense/ Air Force Office of Scientific Research Military Photomedicine Program, department funds (to M.X.W.), and a Bullock-Wellman postdoctoral fellowship (to Q.Z.).

REFERENCES AND NOTES

1. Hallam S, Provan D, Newland AC, Immune thrombocytopenia—What are the new treatment options? Expert Opin. Biol. Ther 13, 1173–1185 (2013). [PubMed: 23682685]
2. Vadhan-Raj S, Management of chemotherapy-induced thrombocytopenia: Current status of thrombopoietic agents. Semin. Hematol 46, S26–S32 (2009). [PubMed: 19245931]
3. Nakeff A, Maat B, Separation of megakaryocytes from mouse bone marrow by velocity sedimentation. Blood 43, 591–595 (1974). [PubMed: 4816846]
4. Kaushansky K, The molecular mechanisms that control thrombopoiesis. J. Clin. Invest 115, 3339–3347 (2005). [PubMed: 16322778]
5. Patel SR, Hartwig JH, Italiano JE Jr., The biogenesis of platelets from megakaryocyte proplatelets. J. Clin. Invest 115, 3348–3354 (2005). [PubMed: 16322779]
6. Patel SR, Richardson JL, Schulze H, Kahle E, Galjart N, Drabek K, Shivdasani RA,Hartwig JH, Italiano JE Jr., Differential roles of microtubule assembly and sliding in proplatelet formation by megakaryocytes. Blood 106, 4076–4085 (2005). [PubMed: 16118321]
7. Richardson JL, Shivdasani RA, Boers C, Hartwig JH, Italiano JE Jr., Mechanisms of organelle transport and capture along proplatelets during platelet production. Blood 106, 4066–4075 (2005). [PubMed: 16118320]
8. Wulfert M, Küpper AC, Tapprich C, Bottomley SS, Bowen D, Germing U, Haas R,Gattermann N, Analysis of mitochondrial DNA in 104 patients with myelodysplastic syndromes. Exp. Hematol 36, 577–586 (2008). [PubMed: 18439489]
9. Houwerzijl EJ, Blom NR, van der Want JJL, Esselink MT, Koornstra JJ, Smit JW,Louwes H, Vellenga E, de Wolf JTM, Ultrastructural study shows morphologic features of apoptosis and para-apoptosis in megakaryocytes from patients with idiopathic thrombocytopenic purpura. Blood 103, 500–506 (2004). [PubMed: 12969975]
10. Morison IM, Cramer Bordé EM, Cheesman EJ, Cheong PL, Holyoake AJ,Fichelson S, Weeks RJ, Lo A, Davies SMK, Wilbanks SM, Fagerlund RD,Ludgate MW, da Silva Tatley FM, Coker MSA, Bockett NA, Hughes G, Pippig DA,Smith MP, Capron C, Ledgerwood EC, A mutation of human cytochrome c enhances the intrinsic apoptotic pathway but causes only thrombocytopenia. Nat. Genet 40, 387–389 (2008). [PubMed: 18345000]
11. Ramsey H, Zhang Q, Brown DE, Steensma DP, Lin CP, Wu MX, Stress-induced hematopoietic failure in the absence of immediate early response gene X-1 (IEX-1, IER3). Haematologica 99, 282–291 (2014). [PubMed: 24056813]
12. Shen L, Zhi L, Hu W, Wu MX, IEX-1 targets mitochondrial F1Fo-ATPase inhibitor for degradation. Cell Death Differ 16, 603–612 (2009). [PubMed: 19096392]
13. Zhi L, Ustyugova IV, Chen X, Zhang Q, Wu MX, Enhanced Th17 differentiation and aggravated arthritis in IEX-1-deficient mice by mitochondrial reactive oxygen species-mediated signaling. J. Immunol 189, 1639–1647 (2012). [PubMed: 22798682]
14. Ramsey H, Zhang Q, Wu MX, Mitoquinone restores platelet production in irradiation-induced thrombocytopenia. Platelets 26, 459–466 (2015). [PubMed: 25025394]
15. Pastore D, Greco M, Passarella S, Specific helium-neon laser sensitivity of the purified cytochrome c oxidase. Int. J. Radiat. Biol 76, 863–870 (2000). [PubMed: 10902741]
16. Zhang Q, Zhou C, Hamblin MR, Wu MX, Low-level laser therapy effectively prevents secondary brain injury induced by immediate early responsive gene X-1 deficiency. J. Cereb. Blood Flow Metab 34, 1391–1401 (2014). [PubMed: 24849666]

17. Gavish L, Asher Y, Becker Y, Kleinman Y, Low level laser irradiation stimulates mitochondrial membrane potential and disperses subnuclear promyelocytic leukemia protein. Lasers Surg. Med 35, 369–376 (2004). [PubMed: 15611960]
18. Dong T, Zhang Q, Hamblin MR, Wu MX, Low-level light in combination with metabolic modulators for effective therapy of injured brain. J. Cereb. Blood Flow Metab 35, 1435–1444 (2015). [PubMed: 25966949]
19. Chen AC-H, Arany PR, Huang Y-Y, Tomkinson EM, Sharma SK, Kharkwal GB, Saleem T,Mooney D, Yull FE, Blackwell TS, Hamblin MR, Low-level laser therapy activates NF-kB via generation of reactive oxygen species in mouse embryonic fibroblasts. PLOS One 6, e22453 (2011). [PubMed: 21814580]
20. Huang Y-Y, Nagata K, Tedford CE, McCarthy T, Hamblin MR, Low-level laser therapy (LLLT) reduces oxidative stress in primary cortical neurons in vitro. J. Biophotonics 6, 829–838 (2013). [PubMed: 23281261]
21. AlGhamdi KM, Kumar A, Moussa NA, Low-level laser therapy: A useful technique for enhancing the proliferation of various cultured cells. Lasers Med. Sci 27, 237–249 (2012). [PubMed: 21274733]
22. Song S, Zhou F, Chen WR, Low-level laser therapy regulates microglial function through Src-mediated signaling pathways: Implications for neurodegenerative diseases. J. Neuroinflammation 9, 219 (2012). [PubMed: 22989325]
23. Elagib KE, Mihaylov IS, Delehanty LL, Bullock GC, Ouma KD, Caronia JF, Gonias SL,Goldfarb AN, Cross-talk of GATA-1 and P-TEFb in megakaryocyte differentiation. Blood 112, 4884–4894 (2008). [PubMed: 18780834]
24. Schulze H, Korpal M, Hurov J, Kim S-W, Zhang J, Cantley LC, Graf T, Shivdasani RA, Characterization of the megakaryocyte demarcation membrane system and its role in thrombopoiesis. Blood 107, 3868–3875 (2006). [PubMed: 16434494]
25. Scarpulla RC, Metabolic control of mitochondrial biogenesis through the PGC-1 family regulatory network. Biochim. Biophys. Acta 1813, 1269–1278 (2011). [PubMed: 20933024]
26. Greene NP, Lee DE, Brown JL, Rosa ME, Brown LA, Perry RA, Henry JN, Washington TA, Mitochondrial quality control, promoted by PGC-1a, is dysregulated by Western diet-induced obesity and partially restored by moderate physical activity in mice. Physiol. Rep 3, e12470 (2015). [PubMed: 26177961]
27. Nguyen LM-D, Malamo AG, Larkin-Kaiser KA, Borsa PA, Adhihetty PJ, Effect of near-infrared light exposure on mitochondrial signaling in C_2C_{12} muscle cells. Mitochondrion 14, 42–48 (2014). [PubMed: 24246911]
28. Raslova H, Roy L, Vourc'h C, Le Couedic JP, Brison O, Metivier D, Feunteun J, Kroemer G,Debili N, Vainchenker W, Megakaryocyte polyploidization is associated with a functional gene amplification. Blood 101, 541–544 (2003). [PubMed: 12393414]
29. Baccini V, Roy L, Vitrat N, Chagraoui H, Sabri S, Le Couedic J-P, Debili N, Wendling F,Vainchenker W, Role of $p21^{Cip1/Waf1}$ in cell-cycle exit of endomitotic megakaryocytes. Blood 98, 3274–3282 (2001). [PubMed: 11719364]
30. Katsman Y, Foo AH, Leontyev D, Branch DR, Improved mouse models for the study of treatment modalities for immune-mediated platelet destruction. Transfusion 50, 1285–1294 (2010). [PubMed: 20088841]
31. Chenaille PJ, Steward SA, Ashmun RA, Jackson CW, Prolonged thrombocytosis in mice after 5-fluorouracil results from failure to down-regulate megakaryocyte concentration. An experimental model that dissociates regulation of megakaryocyte size and DNA content from megakaryocyte concentration. Blood 76, 508–515 (1990). [PubMed: 2378983]
32. Zeuner A, Signore M, Martinetti D, Bartucci M, Peschle C, De Maria R, Chemotherapy-induced thrombocytopenia derives from the selective death of megakaryocyte progenitors and can be rescued by stem cell factor. Cancer Res 67, 4767–4773 (2007). [PubMed: 17510405]
33. Shinjo K, Takeshita A, Nakamura S, Naitoh K, Yanagi M, Tobita T, Ohnishi K, Ohno R, Serum thrombopoietin levels in patients correlate inversely with platelet counts during chemotherapy-induced thrombocytopenia. Leukemia 12, 295–300 (1998). [PubMed: 9529122]

34. Giagkousiklidis S, Vogler M, Westhoff M-A, Kasperczyk H, Debatin K-M, Fulda S, Sensitization for γ-irradiation–induced apoptosis by second mitochondria-derived activator of caspase. Cancer Res 65, 10502–10513 (2005). [PubMed: 16288043]

35. Mostafa SS, Papoutsakis ET, Miller WM, Oxygen tension modulates the expression of cytokine receptors, transcription factors, and lineage-specific markers in cultured human megakaryocytes. Exp. Hematol 29, 873–883 (2001). [PubMed: 11438210]

36. Junt T, Schulze H, Chen Z, Massberg S, Goerge T, Krueger A, Wagner DD, Graf T, Italiano JE Jr.,R. A. Shivdasani, U. H. von Andrian, Dynamic visualization of thrombopoiesis within bone marrow. Science 317, 1767–1770 (2007). [PubMed: 17885137]

37. Parmar K, Mauch P, Vergilio J-A, Sackstein R, Down JD, Distribution of hematopoietic stem cells in the bone marrow according to regional hypoxia. Proc. Natl. Acad. Sci. U.S.A 104, 5431–5436 (2007). [PubMed: 17374716]

38. Zucker-Franklin D, Philipp CS, Platelet production in the pulmonary capillary bed: New ultrastructural evidence for an old concept. Am. J. Pathol 157, 69–74 (2000). [PubMed: 10880377]

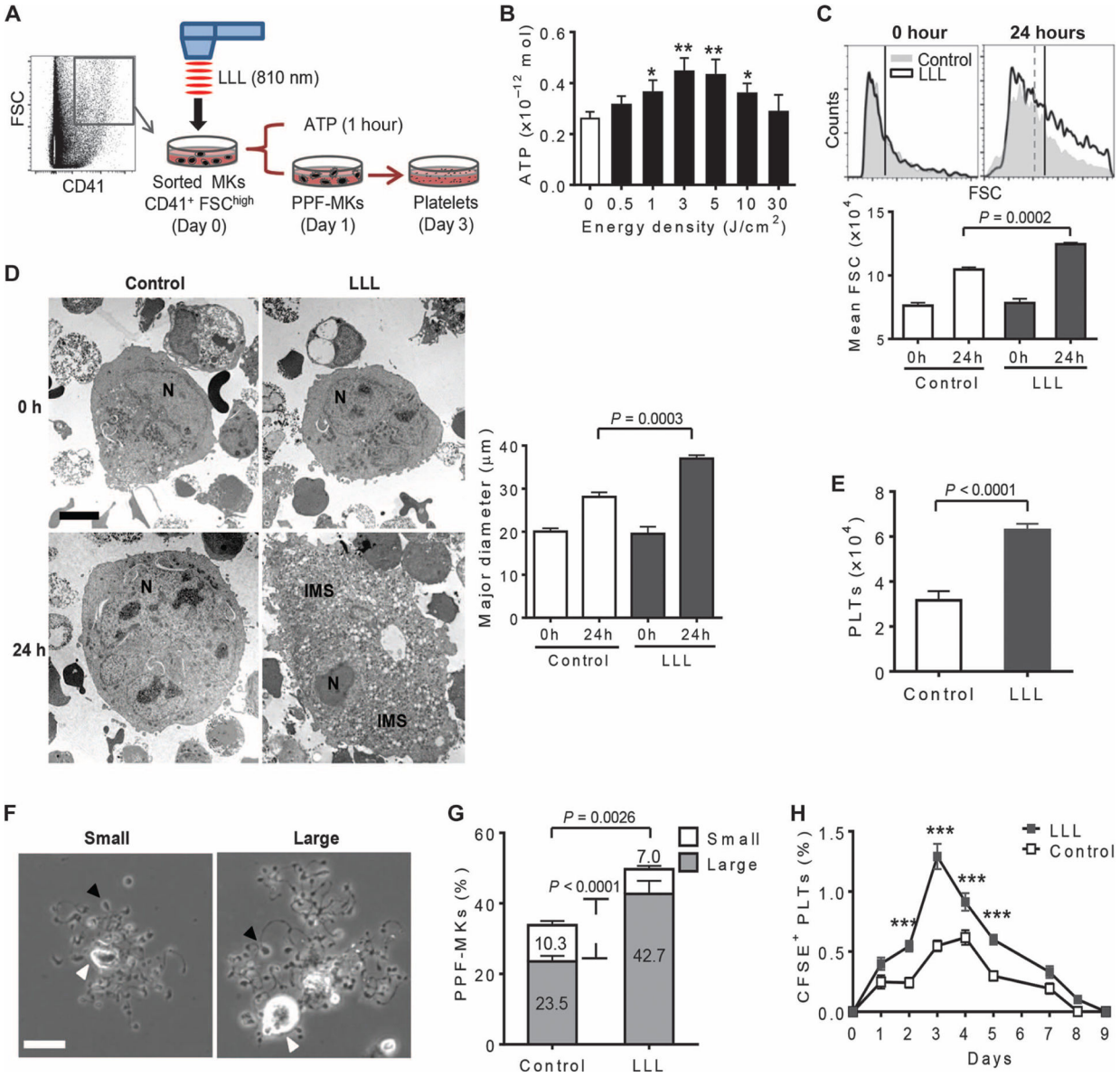

Fig. 1. LLL promotes MK maturation and platelet production.

(**A**) Illustration of timeline for ex vivo platelet differentiation from MKs. CD41$^+$ FSC^{high} MKs were sorted from BMs, treated with or without LLL, and cultured in MK medium. MKs were collected 1 hour later for cellular ATP measurement, 1 day for studying proplatelet formation (PPF), or 3 days for counting platelets. (**B**) ATP was measured in 5 × 10^4 MKs treated with LLL at various energy densities. Data are means ± SEM (n = 6). *P < 0.05, **P < 0.01 versus 0 J/cm^2. (**C**) Sizes of CD41$^+$ MKs were analyzed by flow cytometric analysis of FSC before and after 24-hour differentiation. Data are means ± SEM (n = 6). (**D**) Representative transmission electron micrographs of MKs at 0 and 24 hours after LLL from at least 6 samples per group with 30 cells in each group. Data quantifying the major diameter of MKs are means ± SEM. N, nuclear; IMS, invaginated membrane system. Scale bar, 5 μm. (**E**) The number of platelets (PLTs) derived from 1 × 10^4 MKs was estimated 3 days after LLL on the basis of CD41 expression and FSC/side scatter (SSC). Data are means

± SEM (n = 6). (**F**) Representative images of PPF-MKs at 24 hours after LLL. Small was considered <100 μm, and large was ≥100 μm in PPF-MK diameter. Black arrowheads represent one of many protrusions on proplatelet shafts. White arrowheads indicate the nucleus. Scale bar, 25 μm. (**G**) The percentages of small or large PPF-MKs, as defined in (F), of at least 500 MKs analyzed per sample and 6 samples per group are shown as means ± SEM. (**H**) Sorted MKs were treated with or without LLL, labeled with the fluorophore CFSE, and infused into recipient mice at 1×10^5 cells per mouse. Percentages of resultant $CFSE^+$ platelets in recipients at indicated days are shown. Data are means ± SEM (n = 10). ***$P < 0.001$ compared to controls. P values were determined by one-way analysis of variance (ANOVA) (B to D and H) or two-tailed Student's t test (E and G).

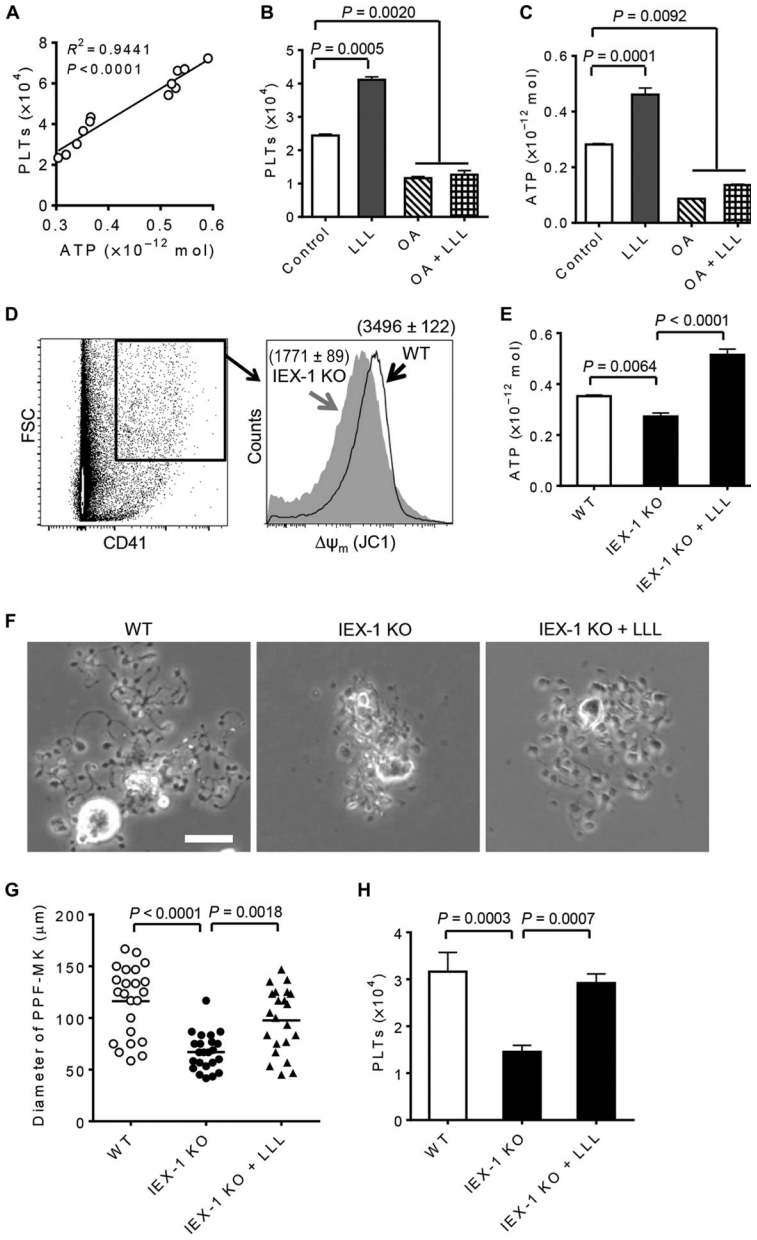

Fig. 2. Thrombopoietic effect of LLL is ATP-dependent.

(**A**) Correlations between MK ATP levels at 1 hour after LLL and platelets measured 3 days later were analyzed ($n = 12$). The coefficient of determination (R^2) and P value were determined by regression and correlation analysis. (**B** and **C**) Effects of LLL on platelet production (B) and ATP synthesis (C) were inhibited by OA (5 μg/ml). Data are means ± SEM ($n = 6$). (**D**) Wild-type (WT) and IEX-1 KO BM nucleated cells were stained with anti-CD41 antibody and JC1. Mitochondrial membrane potential of $CD41^+$ FSC^{high} MKs was determined by flow cytometric analysis of red J-aggregate fluorescence at 590 nm. Data represent three independent experiments. (**E**) Sorted MKs were treated with or without LLL and differentiated for 1 hour before ATP measurement as in Fig. 1B. Data are means ± SEM ($n = 6$). (**F**) Representative images of PPF-MKs were obtained at 24 hours after LLL from at

least 6 samples per group with 25 cells in each group. Scale bar, 25 μm. (**G**) Cell diameters in (F) were shown, each symbol represents a single PPF-MK. (**H**) The number of platelets derived from 1×10^4 MKs was estimated 3 days after LLL on the basis of CD41 expression and FSC/SSC. Data are means ± SEM ($n = 6$). *P* values in (B) to (H) were determined by one-way ANOVA.

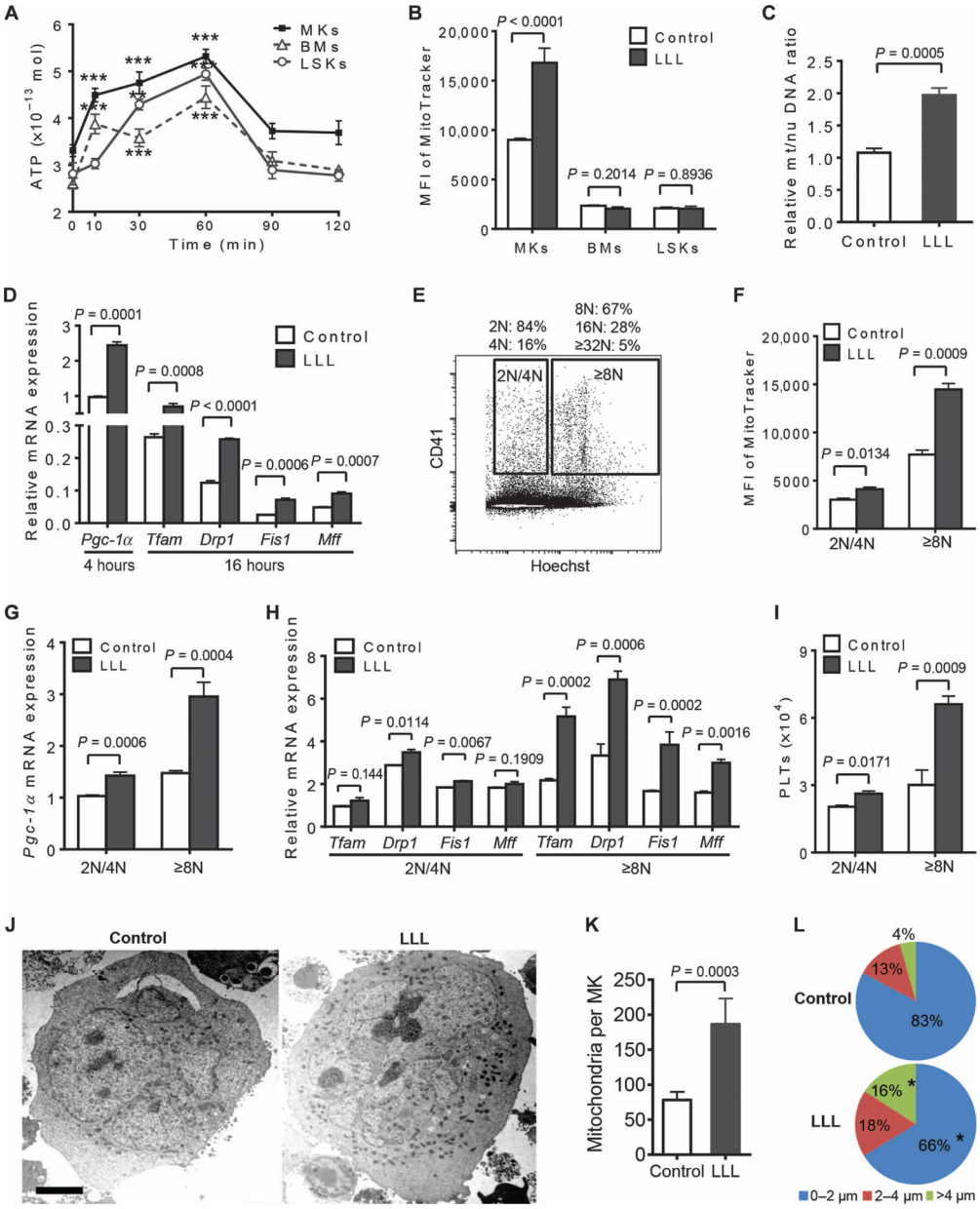

Fig. 3. LLL stimulates mitochondrial biogenesis in polyploid MKs.

(**A**) ATP was measured in MKs, BMs, or LSKs for indicated times after LLL. Data are means ± SEM ($n = 6$). $^{**}P < 0.01$, $^{***}P < 0.001$ versus 0 min. (**B**) At 24 hours after LLL, the indicated cells were stained with MitoTracker and analyzed by flow cytometry. Data are means ± SEM ($n = 6$). MFI, mean fluorescence intensity. (**C**) Mitochondrial (mt) DNA content of MKs was measured by real-time polymerase chain reaction (PCR) and normalized with nuclear (nu) DNA. Data are from three independent experiments with each in triplicate and expressed as means ± SEM. (**D**) *Pgc1a* transcript was measured at 4 hours after LLL, and other gene transcripts were measured at 16 hours after LLL, by quantitative reverse transcription PCR (qRT-PCR). Data are from three independent experiments with each in triplicate and expressed as means ± SEM. (**E** to **I**) MKs were sorted on the basis of

DNA content by staining with Hoechst 33342 and anti-CD41–fluorescein isothiocyanate (FITC) (E), treated with LLL or sham light, and subjected to flow cytometric analysis with MitoTracker 24 hours later (F) or qRT-PCR analysis of *Pgc1a* transcript 4 hours after LLL (G), and other gene transcripts 16 hours after LLL (H). The number of platelets derived from 1×10^4 MKs was estimated 3 days after LLL (I). Data are from three independent experiments with each in triplicate and expressed as means ± SEM. (**J** to **L**) Representative transmission electron micrographs of MKs at 24 hours after LLL. Scale bar, 5 μm. The mitochondrial number of each MK (K) and the shortest distance between each mitochondrion and nearest nuclear region (L) were measured by ImageJ software from at least 30 MKs per group. Data are from three independent experiments with each in triplicate and expressed as means ± SEM. $*P < 0.05$ compared with non-LLL controls. *P* values were determined by one-way ANOVA (A) or two-tailed Student's *t* test (B to L).

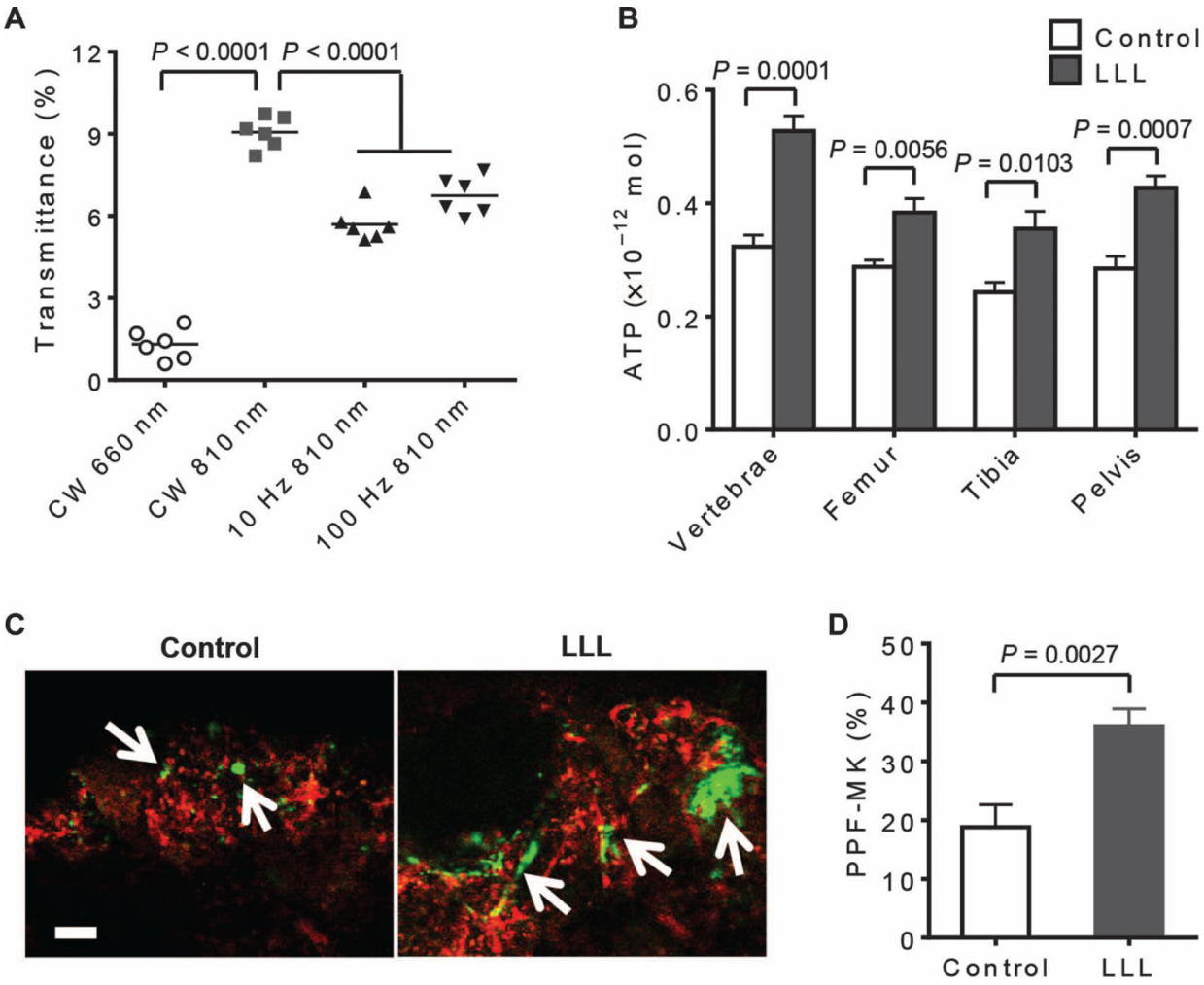

Fig. 4. LLL penetrates into the bones of mice.

(**A**) Transmittance (%) of indicated LLL modes was measured beneath mouse fresh skin and vertebral bones using a laser power meter. Data are means ± SEM ($n = 6$). CW, continuous wave. (**B**) BMs were isolated from indicated bones at 1 hour after whole-body LLL illumination at 30 J/cm^2 to determine ATP levels as in Fig. 1B. Data are means ± SEM ($n = 6$). (**C** and **D**) At 24 hours after whole-body LLL illumination, mice were intravenously injected with anti-CD41–FITC (green) and anti-CD105–phycoerythrin (red) and sacrificed 15 min later. Fresh femurs were then removed from the mice and examined by confocal microscope (C). Arrows indicate MKs. Scale bar, 50 μm. Percentages of PPF-MKs were determined from at least 50 MKs per femur and 6 samples per group (D). Data are from three independent experiments with each in triplicate and expressed as means ± SEM. *P* value was determined by one-way ANOVA (A) or two-tailed Student's *t* test (B and D).

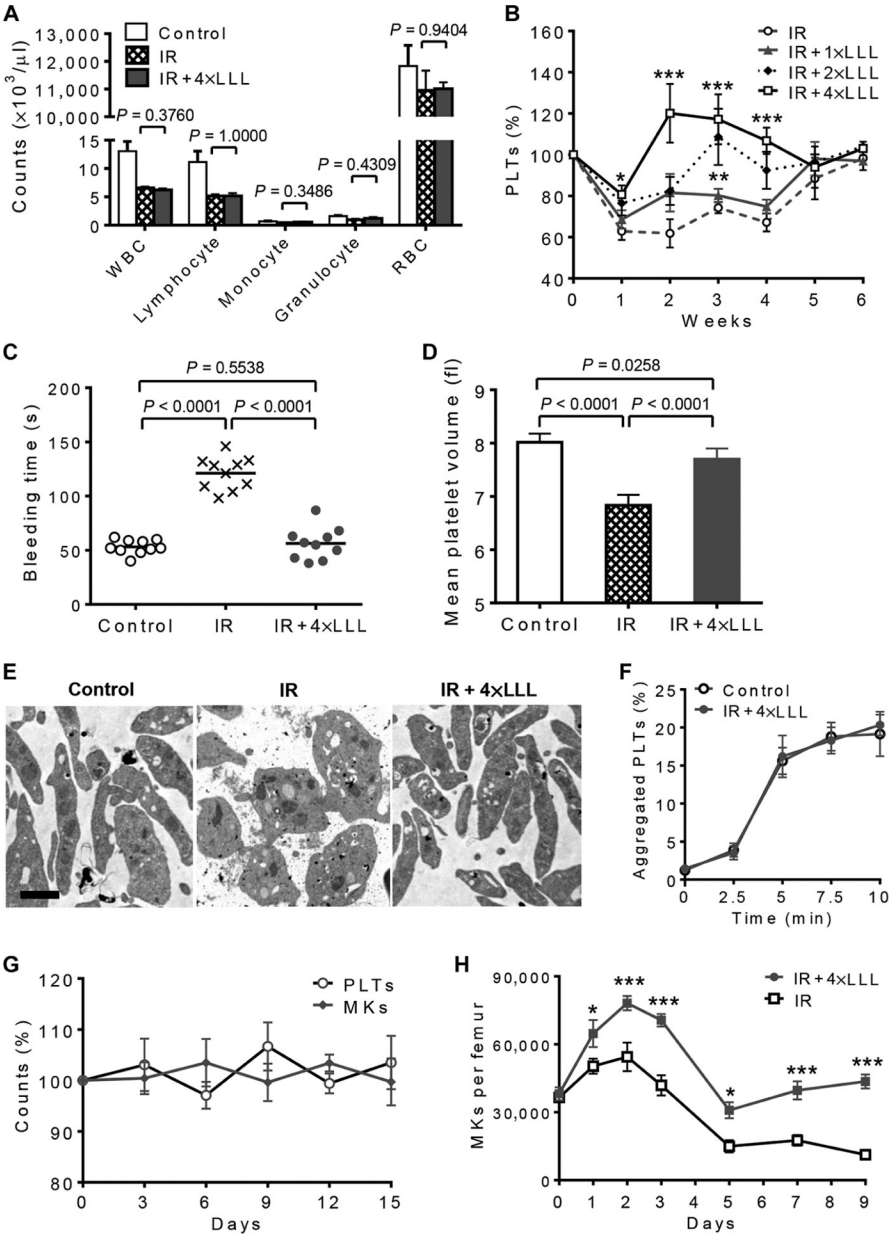

Fig. 5. LLL ameliorates thrombocytopenia induced by IR in vivo.

(**A**) Complete blood counts of white blood cells (WBCs), lymphocytes, monocytes, granulocytes, and red blood cells (RBCs) in 3-Gy γ-irradiated mice 2 weeks after IR. Data are means ± SEM ($n = 15$). (**B**) Platelet counts were obtained at indicated days in 3-Gy γ-irradiated mice (IR), or IR mice treated with LLL once at 6 hours after IR (IR + 1×LLL), once a day on days 0 and 1 (IR + 2×LLL), or once a day from day 0 to day 3 (IR + 4×LLL). Data are means ± SEM ($n = 15$). $^{*}P < 0.05$, $^{**}P < 0.01$, $^{***}P < 0.001$ versus IR. (**C**) The tail bleeding time of each mouse was examined at 2 weeks after IR and presented by individual symbols. (**D**) Platelet volume of each mouse was examined at 2 weeks after IR. Data are means ± SEM ($n = 10$). (**E**) Representative transmission electron micrographs of platelets isolated from indicated mice at 2 weeks after IR. Scale bar, 1 μm. (**F**) Platelets isolated from

non-IR control and IR + 4×LLL mice 2 weeks after LLL were labeled with either anti-CD9 or anti-CD31 antibody, mixed, and stimulated with phorbol 12-myristate 13-acetate (100 ng/ml). Aggregated platelets indicated by double-colored events were quantified by flow cytometry and presented as mean percentages ± SEM ($n = 6$). (**G**) Circulating platelets and BM MKs remain within the steady-state levels in mice treated with LLL at 30 J/cm^2 once every other day for 12 days. Data are mean percentages ± SEM of changes relative to baseline ($n = 6$). (**H**) Effects of four doses of LLL on the number of MKs in γ-irradiated mice over time. Data are mean numbers ± SEM of MKs per femur at indicated days ($n = 6$). *$P < 0.05$, ***$P < 0.001$ comparedwith IR group. P values were determined by two-tailed Student's t test (A and H) or one-way ANOVA (B to D).

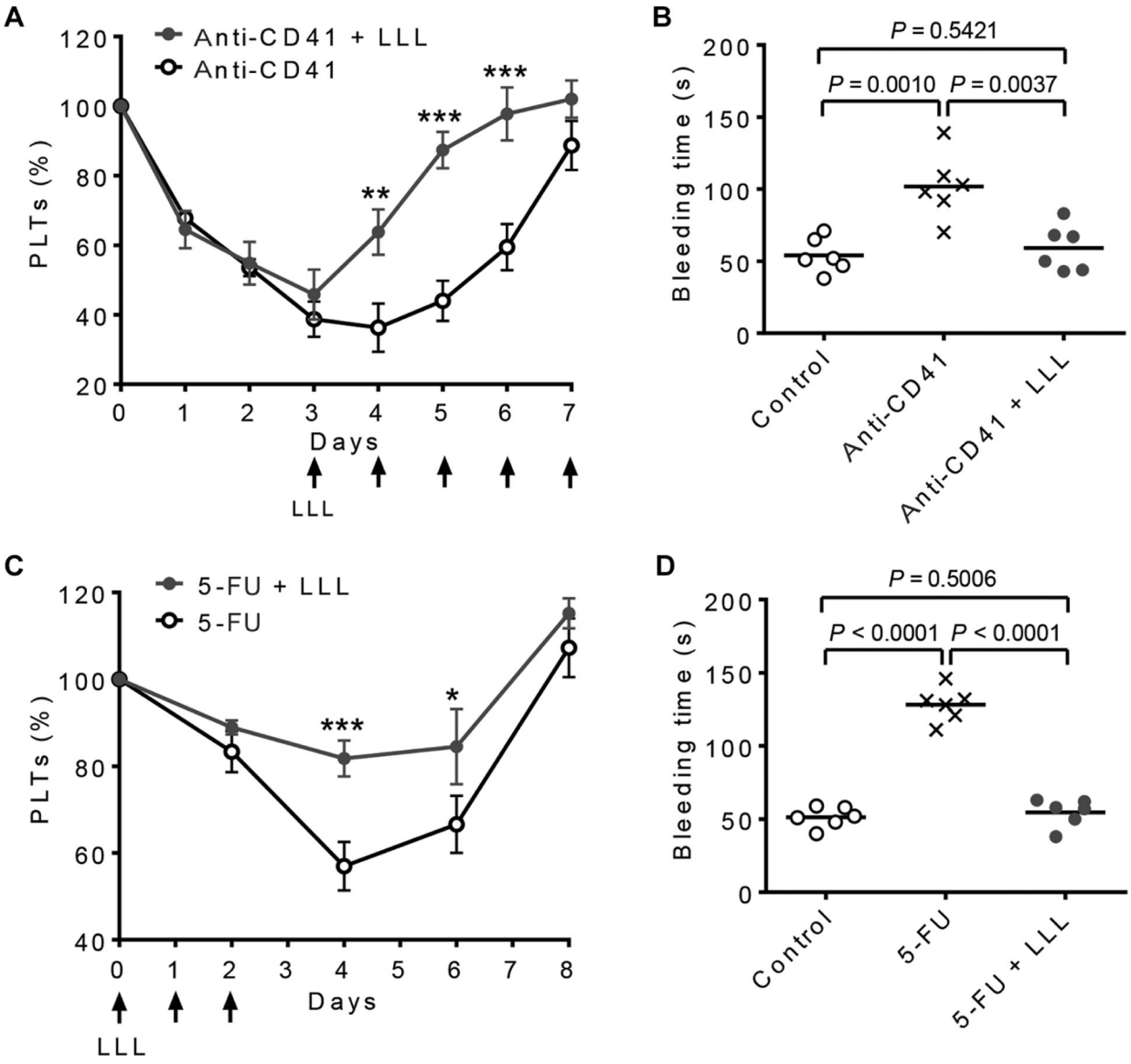

Fig. 6. LLL alleviates thrombocytopenia induced by anti-CD41 antibody or 5-FU in mice.

(**A** and **B**) Mice were administered daily with anti-CD41 antibody (0.1 mg/kg) over 8 days. LLL was given daily from day 3 to day 7 (arrows). (A) Platelet counts were measured daily at 6 hours after LLL. Data are means ± SEM ($n = 6$). (B) Tail bleeding time was examined on day 5. Controls are naïve mice without any treatment. Data are individual animals with mean ($n = 6$). $^{**}P < 0.01$, $^{***}P < 0.001$ versus anti-CD41, unless otherwise noted. (**C** and **D**) Mice were injected with 5-FU (150 mg/kg) on day 0. LLL was given daily for three consecutive days starting at 4 hours after 5-FU injection. (C) Platelet counts were measured daily at 6 hours after LLL. Data are means ± SEM ($n = 6$). (D) Tail bleeding time was examined on day 4. $^{*}P < 0.05$, $^{***}P < 0.001$ versus 5-FU, unless otherwise noted. All P values were determined by one-way ANOVA.

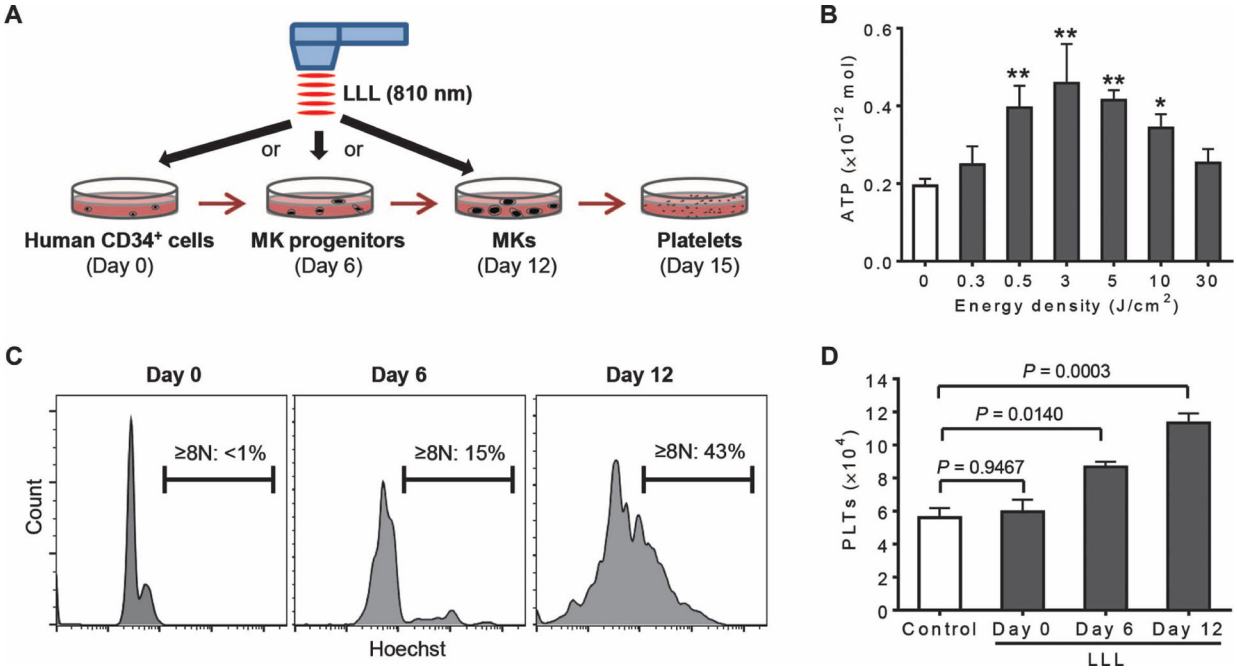

Fig. 7. LLL significantly enhances platelet generation in human MKs.

(**A**) Illustration of timeline for ex vivo platelet differentiation from human $CD34^+$ cells. $CD34^+$ cells differentiated predominantly into MK progenitors in 6 days, MKs in 12 days, and platelets in 15 days. (**B**) ATP was measured in $CD34^+$-derived MKs treated with LLL at various energy densities as in Fig. 1B. Data were obtained from three independent experiments with each in triplicate. $*P < 0.05$, $**P < 0.01$ versus 0 J/cm^2, by one-way ANOVA. (**C**) Ploidy analysis of $CD34^+$ cultures on day 0, 6, or 12 using Hoechst 33342 staining. Data represent three independent experiments. (**D**) LLL at 3 J/cm^2 was administered on day 0, 6, or 12 during $CD34^+$ cell differentiation. Platelets were quantified on day 15 by flow cytometry and expressed as mean numbers ± SEM of platelets derived from 1×10^4 $CD34^+$ cells. Data were obtained from three independent experiments with each in triplicate. *P* values were determined by one-way ANOVA.